

Magnetic and thermal studies of antiferromagnetic linear chains in dichlorobis(pyridine)copper(II)*

William Duffy, Jr. and John E. Venneman†

Department of Physics, University of Santa Clara, Santa Clara, California 95053

Donald L. Strandburg

Department of Physics, California State University at San José, San Jose, California 95192

Peter M. Richards‡

Sandia Laboratories, Albuquerque, New Mexico 87115

(Received 15 October 1973)

Results of static-susceptibility measurements from 1.5 to 300 K, heat-capacity studies from 0.5 to 10 K, and room-temperature 8.8-GHz EPR measurements are presented for dichlorobis(pyridine)copper(II), a spin-1/2 antiferromagnetic linear-chain crystal. The Bonner-Fisher chains curve gives good agreement with the measured susceptibility values from 2 K to room temperature, for $J/k_B = -13.4 \pm 0.2$ K and $g = 2.07 \pm 0.04$. The heat capacity exhibits a sharp anomalous peak at 1.130 ± 0.005 K, corresponding to an antiferromagnetic-paramagnetic transition at that temperature. From 4–8 K, the heat capacity is resolved into a T^3 lattice contribution with $\Theta_D = 82.2 \pm 2$ K and a Bonner-Fisher chains curve with $J/k_B = -13.2 \pm 0.3$ K. Principal-axis g values and the orientation of the principal axes with respect to the crystalline axes were determined. The two inequivalent copper ions exhibit only a single resonance line at 8.8 GHz, because of interchain exchange narrowing. The EPR line is found to be Lorentzian out to seven absorption halfwidths. Theoretical line shapes are compared with the experimental data for various estimates of interchain exchange. The Tahir-Kheli decoupling-theory estimate of nearest-interchain-neighbor exchange integral of 0.051 K gives best agreement with the observed line-shape data.

INTRODUCTION

One-dimensional exchange-coupled spin systems have been the subject of intensive theoretical and experimental investigation in recent years. Theoretical discussions have often focused on *isolated* linear-chain systems, while experimental results often exhibit residual interchain effects, since the available crystalline systems are three-dimensional in spatial character. The profound effect on the equilibrium thermodynamic properties of even very small residual interchain exchange has been appreciated since the famous Onsager calculation of the specific heat of the two-dimensional Ising net.^{1,2} Only very recent work has elucidated the equally profound effects of interchain exchange on the spin dynamics, as observed experimentally by electron-spin-resonance studies of dichlorobis(pyridine)copper(II), tetraamminecopper(II) sulphate monohydrate, the α form of bis(N-methylsalicylal-diminato)copper(II), and cesium manganese chloride dihydrate.^{3,4}

Dichlorobis(pyridine)copper(II) has been identified as a spin- $\frac{1}{2}$ Heisenberg antiferromagnetic linear-chain salt in which the residual interchain exchange has been thought to be very small compared to the intrachain exchange, as evidenced by measurements of crystal structure,⁵ magnetic susceptibility,⁶ low-temperature magnetization,⁷ magnetic specific heat,⁶ and electron-spin resonance.^{3,4}

The experimental study described in this paper provides new information on both intrachain and interchain exchange interactions in this quasi-one-dimensional system, and provides both confirmation and contradiction of important aspects of earlier work.

Dichlorobis(pyridine)copper(II), less correctly but commonly named copper dipyridine dichloride, will be abbreviated CPC in this paper. The crystal structure⁵ is monoclinic, with space group $P2_1/n$, and with two formula units in the unit cell. Each copper ion is located at the center of a nearly equilateral parallelogram (rhombus) with nearest-neighbor chlorine ions and pyridine nitrogens at alternate vertices. The rhombuses are stacked along the c axis, as shown in Fig. 1(a). The normal to each rhombus is at an angle of 36.1° to the c axis. This arrangement in the chain results in rhombic local symmetry for the copper ion, surrounded as it is by two in-rhombus chlorines at 2.28 Å, two in-rhombus nitrogens at 2.02 Å, and two next-nearest-neighbor chlorines on adjacent rhombuses in the stack, at 3.05 Å, and on a line which is almost orthogonal to the central rhombus. The intrachain nearest-neighbor copper ions are separated by 3.87 Å as compared to the nearest-neighbor interchain separation of 8.59 Å. There are two mirror-image related chains corresponding to the two formula units in the unit cell. The symmetry operation of glide reflection along $\frac{1}{2}\vec{a} + \frac{1}{2}\vec{c}$

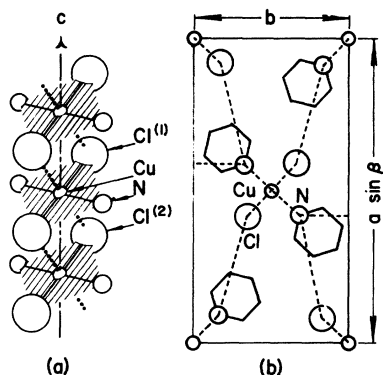


FIG. 1. Structural features of CPC crystal. (a) The chain of Cu^{++} ions; (b) view of the unit cell normal to the chain axis (the c axis), with likely superexchange paths indicated by dashed lines.

convert the chains into each other.

The structure within the individual chains in CPC is very similar to that in the chains of the much-studied crystal $\text{CuCl}_2 \cdot 2\text{H}_2\text{O}$.⁸ In Table I the significant lattice spacings of the similar crystals are listed and may be compared. The hydrated cupric chloride chains are isomorphic with the CPC chains except that the water molecules replace the pyridines, and some interatomic separations are slightly larger in CPC.

The positioning of the two inequivalent chains in the crystal of the hydrated cupric chloride is such that the CuCl_2 groups in a given chain all lie in a plane normal to a given crystalline axis which results in a g^2 tensor with principal axes along the crystalline axes. The CuCl_2 molecular units in a single chain of the CPC lie in planes which are canted to the a and b axes. The presence of the large pyridine rings projecting out from the sides of the chains, as seen in Fig. 1(b), leads to a much larger interchain separation than results from the water molecules, yielding much smaller interchain exchange in CPC than in $\text{CuCl}_2 \cdot 2\text{H}_2\text{O}$.

The small blue needle-shaped crystals of CPC were grown following the methods described by Takeda, Matsukawa, and Haseda.⁶ Static susceptibility and specific-heat measurements were performed on polycrystalline material. Electron-spin-resonance measurements were performed on a single needle, which was shown to be a single crystal by x-ray diffraction techniques.

MAGNETIC SUSCEPTIBILITY

The susceptibility measurements were performed in a Faraday susceptometer using an electric balance similar to the one described by McGuire and Lane.⁹ The typically 100-mg sample is suspended from the balance by a quartz fiber in a field of

TABLE I. Lattice parameters and nearest-neighbor separations in CPC and $\text{CuCl}_2 \cdot 2\text{H}_2\text{O}$ as obtained from Refs. 5 and 8.

	CPC	$\text{CuCl}_2 \cdot 2\text{H}_2\text{O}$
Space group	$P2_1/n$	Pbmn
a (Å)	17.00	7.38
b (Å)	8.59	8.04
c (Å)	3.87	3.72
β	$91^\circ 52'$	90°
Cu-Cu, intrachain (Å)	3.87	3.72
Cu-Cl ⁽¹⁾ (Å)	2.28	2.28
Cu-Cl ⁽²⁾ (Å)	3.05	2.94
Cu-N (Å)	2.02	...
Cu-O (Å)	...	5.56
Cu-Cu, interchain (Å)	8.59	5.46

about 5 kOe, surrounded by helium heat-exchange gas at a pressure of about 1 Torr. Germanium- and copper-resistance thermometry are used in the temperature ranges of 1–40 K and 40–300 K, respectively. Additional details of the apparatus are given in earlier publications.^{10,11} Absolute susceptibilities are determined from measurements on a Pt standard, taking the room-temperature susceptibility of Pt to be 0.968×10^{-6} emu/g.

The measured susceptibility of polycrystalline CPC is shown in Fig. 2. Also shown are the data of Takeda *et al.*,⁶ which generally are in good agreement with our results. In order to obtain the temperature-dependent paramagnetic component, diamagnetic and temperature-independent paramagnetic terms must be subtracted from the experimental values. The diamagnetism is estimated to be -159×10^{-6} emu/mole, and the temperature-independent paramagnetism is estimated to be 73

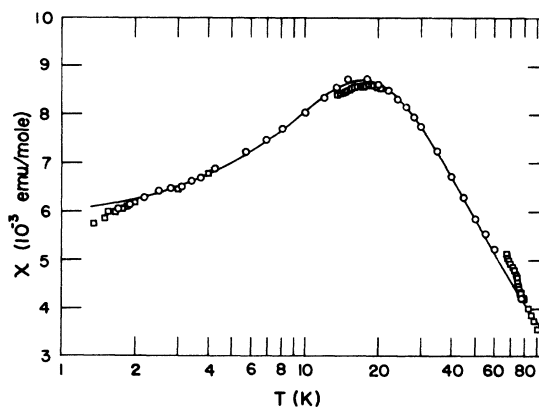


FIG. 2. Magnetic susceptibility of CPC vs temperature. The squares are the data of Takeda, Matsukawa, and Haseda (Ref. 6). The curve is the theoretical linear-chain result of Bonner and Fisher (Ref. 13) corresponding to $J/k_B = -13.4 \pm 0.2$ K and $g = 2.07 \pm 0.04$.

TABLE II. Heat capacity of CPC from 0.5 to 10 K.

T (K)	C (J/mole K)	T (K)	C (J/mole K)	T (K)	C (J/mole K)
0.576	0.0657	1.154	0.416	4.24	1.330
0.633	0.0845	1.180	0.390	4.51	1.485
0.674	0.0989	1.222	0.378	4.73	1.602
0.737	0.1259	1.242	0.375	4.99	1.758
0.780	0.1536	1.264	0.374	5.31	2.013
0.819	0.1775	1.303	0.379	5.58	2.144
0.865	0.2129	1.344	0.383	5.87	2.361
0.896	0.2449	1.405	0.394	6.08	2.451
0.928	0.2717	1.497	0.412	6.27	2.663
0.957	0.306	1.596	0.434	6.53	2.764
0.978	0.329	1.696	0.459	6.74	3.03
0.990	0.347	1.787	0.485	7.03	3.17
1.008	0.375	1.936	0.533	7.26	3.30
1.032	0.416	2.172	0.598	7.37	3.45
1.040	0.430	2.272	0.628	7.49	3.56
1.056	0.460	2.390	0.657	7.74	3.72
1.074	0.500	2.483	0.688	8.00	4.17
1.083	0.548	2.653	0.737	8.20	4.19
1.096	0.568	2.862	0.800	8.36	4.37
1.098	0.578	3.087	0.859	8.65	4.67
1.103	0.589	3.243	0.914	8.75	4.85
1.113	0.653	3.400	0.972	9.20	5.29
1.118	0.695	3.494	1.008	9.69	5.82
1.123	0.748	3.705	1.080	9.79	6.00
1.134	0.755	3.865	1.153	10.27	6.35
1.139	0.605	4.024	1.223	10.35	6.58

$\times 10^{-6}$ emu/mole using the crystal-field splitting of $10Dq$ equal to $14\,285\text{ cm}^{-1}$ as measured by König and Schläfer.¹² The net temperature-independent correction is only about 1% at the temperature of the susceptibility maximum.

The Heisenberg antiferromagnetic linear-chain susceptibility calculated by Bonner and Fisher¹³ has been fitted to the temperature-dependent paramagnetic component of the data. The system Hamiltonian is given by

$$\mathcal{H} = \sum_i (-2J\vec{S}_i \cdot \vec{S}_{i+1} + g\mu_B H S_{iz}), \quad (1)$$

where J is the nearest-neighbor-exchange integral, \vec{S}_i is the spin on the i th site along the chain, g is the (assumed) isotropic g factor, μ_B is the Bohr magneton, and H is the external magnetic field directed along the z axis. As seen in Fig. 2, the data are in excellent agreement with the Bonner-Fisher curve over an absolute temperature range of about two decades. The fitting parameters correspond to $J/k_B = -13.4 \pm 0.2\text{ K}$ and $g = 2.07 \pm 0.04$, where k_B is Boltzmann's constant. As noted by Takeda *et al.*,⁶ there is a clear deviation from the Bonner-Fisher curve below about 2 K, which is attributable to the onset of short-range ordering associated with interchain effects as the vicinity of the transition temperature is approached. As discussed further on, our calorimetric study shows that the transition temperature is 1.13 K.

HEAT CAPACITY

The heat capacity was measured in the temperature range of 0.5–10 K in an adiabatic calorimeter of conventional design. The 400-mg polycrystalline sample of CPC was sealed in the copper calorimeter can with He³ heat exchange gas at a pressure of 35 Torr. Temperatures were measured with a Scientific Instruments germanium thermometer. The addenda correction was determined directly in a separate measurement. Additional details of the measurement system are given in earlier publications.^{10,11}

The experimental data are given in Table II and plotted below 4 K in Fig. 3. Also shown in the figure are the data of Takeda *et al.*,⁵ which agree rather well with our data in the entire range of overlap. The CPC heat capacity C was resolved into lattice heat capacity C_L and magnetic heat capacity C_M . The quantity $C - C_M(J)$ was least-squares fitted to a T^3 curve for various choices of temperature ranges and J values, where $C_M(J)$ is the theoretical Heisenberg linear-chain result of Bonner and Fisher.¹³ The temperature range over which this fit might be expected to be appropriate is limited on the low side by expected deviations from $C_M(J)$ because of interchain interactions as the transition temperature is approached, and limited on the high side by expected lattice heat-capacity deviations

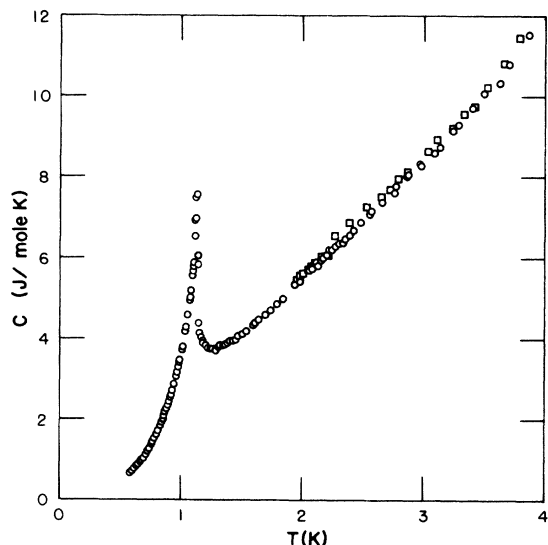


FIG. 3. Low-temperature heat capacity of CPC vs temperature. The squares are the data of Takeda, Matsukawa, and Haseda (Ref. 6). The transition temperature is 1.130 ± 0.005 K.

from the T^3 law. Mindful of these limitations, a temperature range of 4.02–8.00 K was selected. The minimum-standard-deviation fit of $C_M - C(J)$ yielded a value of $J/k_B = -13.2 \pm 0.3$ K. A plot of the fitted curve is shown in the inset in Fig. 4. The corresponding lattice heat capacity was found to be $C_L = 0.00350T^3$ J/mole K, giving a Debye temperature Θ_D of 82.2 ± 2 K. When the data of Takeda *et al.*⁶ were similarly analyzed over the same range of temperatures, the best fit to the data corresponded to $J/k_B = -13.2$ K and $\Theta_D = 80.3$ K.

Some idea of the reliability of the calculated values of J/k_B and Θ_D may be inferred from the listing of values for different ranges of temperature given in Table III. Because of a slope change of C in the vicinity of 3.5 K, data below 4 K were excluded from the fit temperature range since no corresponding slope-change occurs in the result of Bonner and Fisher. The 4–8-K fit was chosen as *most reliable* based on using all data above 4 K and below about $0.1\Theta_D$. Increased standard deviation with increased temperature range, seen in Table III, is associated with the increased scatter in higher-temperature data because of decreased thermometer sensitivity. The excellent fit of $C - C_M (-13.2k_B)$ to the T^3 law, as seen in the inset of Fig. 4, is taken to be good evidence for the correctness of our analysis procedure. In addition, we note the good agreement of our *most reliable* J/k_B value of -13.2 K with the more precisely determined susceptibility value of -13.4 K.

The magnetic-heat-capacity data plotted in Fig.

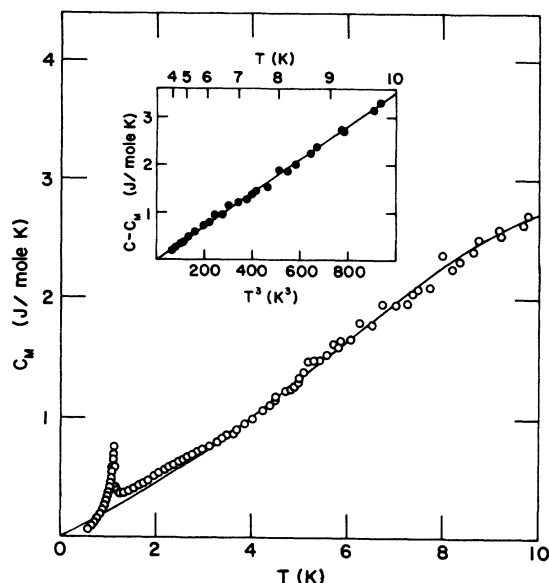


FIG. 4. Magnetic heat capacity of CPC vs temperature. The smooth curve is the theoretical linear-chain result of Bonner and Fisher (Ref. 13) corresponding to $J/k_B = -13.2$ K. The inset shows the difference between total and magnetic heat capacities vs the cube of the temperature.

4 were obtained by subtracting the $0.00350T^3$ value of C_L from each measured value of C . The smooth curve shown is the Bonner-Fisher magnetic heat capacity for $J/k_B = -13.2$ K. Deviations from this linear-chain curve below about 3 K are clearly resolved and may be attributed to interchain short-range ordering as the transition temperature T_N is approached from the high-temperature side. The Néel temperature T_N was found to be 1.130 ± 0.005 K.¹⁴

From our knowledge of J and T_N , it is possible to obtain reasonable estimates for the interchain exchange interactions, which must be present to account for the long-range-order transition at T_N . Each copper ion has two nearest interchain neighbors at 8.59 Å and eight next-nearest interchain neighbors at 9.72 Å. The likely Cu-Cl-N-Cu superexchange paths are nearly identical for the two nearest interchain neighbors and four of the next-

TABLE III. Minimum-standard-deviation fitting constants for CPC heat-capacity data for different choices of temperature range. The underlined values are believed to be *most reliable*, as explained in the text.

Temp. range (K)	J/k_B (K)	Standard deviation	Θ_D (K)
4.02–7.03	-13.4	0.035	80.6
4.02–7.74	-13.0	0.040	83.4
4.02–8.00	<u>-13.2</u>	0.045	<u>82.2</u>
4.02–9.18	-13.2	0.045	82.3
4.02–10.27	-13.1	0.050	82.7

nearest interchain neighbors. There is an appreciably longer superexchange path to the remaining four next-nearest interchain neighbors. It is thus reasonable to assume *equal* interchain interaction j with *six* interchain neighbors, as indicated by the dashed lines in Fig. 1(b).

Various Green's-function calculations of T_N show it to be a function of the product $zJ'(z)$, where z is the number of *interchain* nearest neighbors and $J'(z)$ is the nearest-interchain-neighbor exchange integral. Following Hennessy, McElwee, and Richards,⁴ we make use of this dependence to adapt theoretical results for the orthorhombic lattice with $z = 4$ to this system where $z = 6$. For a given T_N , we may write

$$4J' = 6j, \quad (2)$$

where J' is the equivalent exchange integral corresponding to equal interchain interactions with *four* nearest neighbors lying in a square configuration in a plane normal to the chain axis.

The Green's-function predictions for T_N , in terms of J and J' , may be given in the form

$$k_B T_N / J = f / I, \quad (3)$$

where f is a factor depending on the decoupling employed, and I is an integral dependent on spin, J , J' , and the assumed nearest-neighbor arrangement. The integral I has been evaluated by Montroll¹⁵ for the orthorhombic lattice, with interchain exchange J' with each of four neighbors, and he finds for spin- $\frac{1}{2}$ that

$$I = 0.64J/J', \quad (4)$$

if $J'/J \ll 1$. In the random-phase approximation, $f = 1$; from the Callen decoupling calculation, $f = 2I - 1$ ¹⁶; and according to Tahir-Kheli's decoupling calculation, $f = (2I + 1)/(3I)$.¹⁷

In Table IV the estimates of these various theories for J' are given, together with the corresponding results for the spin- $\frac{1}{2}$ linear-chain salt tetra-aminocopper (II) sulphate monohydrate (CTS),

TABLE IV. Néel temperature T_N , and intrachain coupling J , with corresponding estimates of interchain coupling J' , for CPC and CTS. The estimates of J' are determined by the random-phase approximation (RPA), the Callen calculation (C), and the Tahir-Kheli method (TK).

	T_N (K)	J/k_B (K)	RPA	$10^3 J'/J$ C	TK
CPC	1.13	-13.4	2.9	0.8	5.8
CTS	0.43 ^a	-3.15 ^b	7.6	2.1	14.4

^aS. Saito, J. Phys. Soc. Jap. **26**, 1388 (1969).

^bT. Haseda and A. R. Miedema, Physica (Utr.) **27**, 1102 (1961); R. Griffiths, Phys. Rev. **135**, A659 (1964).

TABLE V. Measured principal-axis g values and axis orientations. The angle θ is measured in the a - c plane with $\theta = 0^\circ$ along the c axis and $\theta = \beta = 91^\circ 52'$ along the a axis.

	g value	Axis orientation	Previously published results
g_1	2.061	$\theta = 62^\circ$	2.062, ^a 2.059 ^b
g_2	2.084	b axis	2.085, ^a 2.059 ^b
g_3	2.220	$\theta = -28^\circ$	2.200, ^a 2.228 ^b

^aV. F. Anufrienko, A. P. Terent'ev, E. G. Rukhadze, and A. G. Onuchina, Teor. Eksp. Chem. **2**, 313 (1966).

^bO. Constaninescu, I. Pascaru, and E. Segal, Rev. Roumaine Chem. **16**, 1493 (1971).

which have previously been calculated by Hennessy *et al.*⁴ When values of J'/J for CPC and CTS are compared, it is clear that CPC chains are *more isolated* from their neighbors than those in the now-classic linear-chain salt CTS.

ELECTRON-SPIN RESONANCE

The ESR measurements were performed at room temperature in an X-band spectrometer at 8.8 GHz. The spectrometer is a conventional reflection homodyne system utilizing 15-kHz field modulation and phase-sensitive detection using a PAR HR-8 lock-in amplifier. The klystron signal source is frequency locked to the Varian V-4531 sample cavity. More than adequate field homogeneity and stability are provided by a Varian V-4007 6-in. magnet with V-3754 cylindrical ring-shim pole caps and a V-2200A power supply. The magnetic field was monitored by a proton resonance probe, and the microwave frequency was measured with a Hewlett-Packard HP524B counter and HP540A transfer oscillator. The counter time base was standardized against the NBS standard-frequency broadcasts.

The g value of CPC was measured on a single crystal as a function of angular position in the b - c and a - c planes and in a plane normal to the c axis. The angular dependence of g^2 agreed very well with the usual expected functional form. Least-squares fit of g^2 as a function of angular position in each of the orthogonal planes were used to obtain the elements of the g^2 tensor, which was then diagonalized to obtain the principal values and axes. In Table V the principal g values and the corresponding principal axes are listed, as well as values determined by measurements on polycrystalline samples by other authors.

The powder g value of 2.07 ± 0.04 determined from the static susceptibility results may be compared with the powder-value based on the EPR results of $[\frac{1}{3}(g_1^2 + g_2^2 + g_3^2)]^{1/2}$ equal to 2.123. The

small discrepancy may be attributable to (i) lack of orientational homogeneity in the polycrystalline sample because of the needlelike character of the crystals; (ii) temperature dependence of the g value, since the susceptibility result derives from low-temperature data while the EPR result is from room-temperature data; or (iii) a combination of (i) and (ii).

In no crystal orientation was there any evidence of the two lines that one might anticipate, corresponding to the two inequivalent positions of the formula units in the unit cell. Apparently, there is sufficient exchange interaction between neighboring inequivalent chains to narrow the contributions from the two into a single ESR line at all orientations. If this interpretation is valid, one can calculate the g values of the individual sites in terms of the measured g values and the angle 2α between the local symmetry axes of the two inequivalent formula unit positions.¹⁸ The two inequivalent formula units and the corresponding chains are mirror images of each other in the a - c plane. This symmetry leads to site g^2 tensors with the same principal values but principal axes which are mirrored images of each other in the a - c plane. If, as a first approximation to the rhombically distorted octahedral symmetry about each copper, one assumes tetragonally distorted octahedral symmetry, rather simple relations may be written to relate the site g^2 tensors to the crystal g^2 tensor. Thus,

$$\begin{aligned} g_1^2 &= g_1^2, \\ g_2^2 &= g_1^2 \cos^2 \alpha + g_{\parallel}^2 \sin^2 \alpha, \\ g_3^2 &= g_1^2 \sin^2 \alpha + g_{\parallel}^2 \cos^2 \alpha, \end{aligned} \quad (5)$$

where $g_1 < g_2 < g_3$ are the principal-axis g values, previously listed in Table II; g_1 and g_{\parallel} are the *site*

g values with respect to the local tetragonal axis; and 2α is the angle between the tetragonal axes of the two inequivalent sites. Using the measured crystal principal-axis values, one obtains $g_1 = 2.061$, $g_{\parallel} = 2.242$, and $\alpha = 20.7^\circ$. The value for α is in rather good agreement with the 23.3° half-angle between the Cu-Cl⁽²⁾ directions of the two inequivalent sites.

For the magnetic field oriented along the direction of a site principal axis corresponding to g_{\parallel} , the difference in g values Δg of the inequivalent sites is given by

$$\Delta g = (g_{\parallel} - g_1) \sin^2 2\alpha. \quad (6)$$

This corresponds to a difference in resonance fields of 120 Oe, and may be compared with the observed peak-to-peak derivative linewidths which ranged from 13.5 to 20 Oe, depending on crystal orientation. Clearly, there must be exchange narrowing of the lines from the two sites into a single line. For this narrowing to occur, we would expect $2j/k_B$ to be at least equal to the Zeeman separation corresponding to the Δg of Eq. (6). According to Eq. (2) and Table IV, estimates of $2j/k_B$ range from 0.03 to 0.23 K. These values are equal to or greater than the Zeeman energy separation of the inequivalent sites of 0.03 K, or less, depending on the field direction.

The results of our line-shape measurements are shown in Fig. 5. The data are plotted in a form which yields a straight line for a Lorentzian line shape. The abscissa $(\Delta H)^2$ is the square of the difference between the field and the field at resonance. The ordinate is the square root of the ratio of ΔH to the absorption derivative g' , with this square root normalized to unity at the center of the line. Within experimental accuracy, the data corresponds to Lorentzian line shapes out to seven ab-

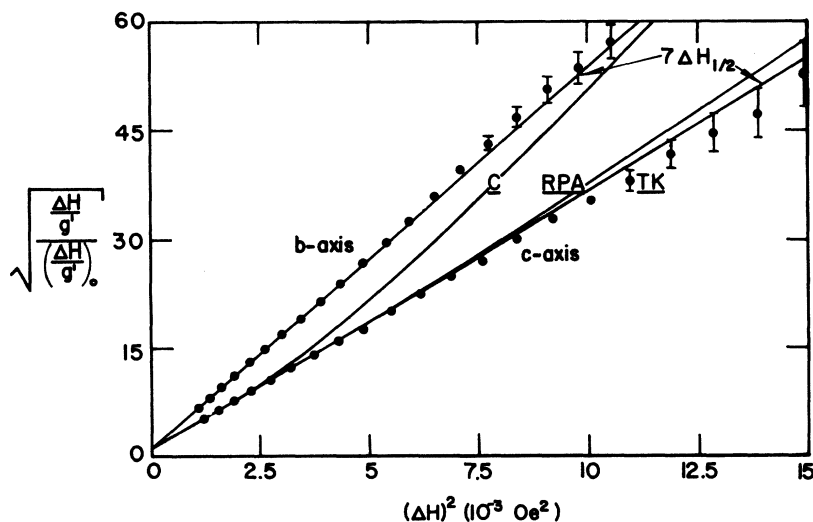


FIG. 5. ESR absorption derivative spectrum of CPC, along the b and c axes. The coordinates have been chosen to yield a straight line for a Lorentzian absorption. The data shown are averaged values for two independent sweeps through the resonance using averaged low- and high-field data. Curves labeled C, RPA, and TK correspond to the theoretical estimates of interchain exchange based on the theories of Callen, the random-phase approximation, and Tahir-Kheli, respectively.

TABLE VI. Values of the one-dimensional rate constant γ and the characteristic time t_0 for $\Delta H_{1/2} = 16.9$ Oe corresponding to the different theoretical estimates of J'/J .

	$10^3 J'/J$	γ (s^{-1})	t_0 (s)
Callen theory	0.8	2.73×10^8	8.91×10^{-9}
RPA	2.9	4.27×10^8	1.60×10^{-9}
Tahir-Kheli theory	5.8	5.72×10^8	6.35×10^{-10}

sorption half-widths. The absorption half-widths $\Delta H_{1/2}$ have been found by fitting the data for small $(\Delta H)^2$ to the Lorentzian equation

$$\left[\frac{(\Delta H)}{g'} \right] / \left[\frac{(\Delta H)}{g'} \right]_0^{1/2} = 1 + \left(\frac{\Delta H}{\Delta H_{1/2}} \right)^2 \quad (7)$$

Bartkowski *et al.*³ and Hennessey *et al.*⁴ have reported finding markedly *non-Lorentzian* line shapes in EPR measurements on CPC. Recent unpublished data by Hennessey on a single crystal confirm our result of Lorentzian character out to ten half-widths.¹⁹ The earlier data may be erroneous due to some problem associated with the polycrystalline character of the sample.

In several recent papers, Richards and co-workers^{20,3,4} have presented a theory of the line shape of one-dimensional exchange-coupled spin systems in the case where some small interchain exchange-interaction is present. The line shape is given by the Fourier transform of a relaxation function $\phi(t)$, which describes the time decay of the transverse magnetization in the frame rotating at the resonance frequency. For isolated chains ($J' = 0$), the relaxation function is $\exp -(\gamma t)^{3/2}$, where γ is a rate constant related to the one-dimensional absorption half-width at half-maximum $\Delta \tilde{H}_{1/2}$ by

$$\Delta \tilde{H}_{1/2} = 1.439 \gamma / \gamma_e \quad (8)$$

where γ_e is the electron gyromagnetic ratio. For J' nonzero, but small compared to J , the relaxation function $\exp[-(\gamma t)^{3/2}]$ persists only for times small compared to some characteristic time t_0 , which measures how long it takes for interchain exchange to affect the magnetization. For times large compared to t_0 , interchain effects lead to a decaying exponential dependence on time. According to Hennessey *et al.* for $S = \frac{1}{2}$, the characteristic time t_0 is given by

$$t_0 = \left(\frac{3}{8} \right)^{2/3} \left(\frac{2\pi D}{c^2} \right)^{1/3} \left(\frac{J'}{\hbar} \right)^{-4/3} \quad (9)$$

where D is the one-dimensional diffusion constant. Inserting the Tahir-Kheli-McFadden²¹ result for D into Eq. (9), we obtain

$$t_0 = \sqrt{\pi} \left(\frac{9}{32} \right)^{1/3} \left(\frac{J}{J'} \right)^{1/3} \left(\frac{\hbar}{J'} \right) \quad (10)$$

The relaxation function $\phi(t)$ may be regarded as a function of the one-dimensional rate constant γ and the characteristic interchain time constant t_0 . Alternately, the $\phi(t)$ may be regarded as a function of the absorption half-width at half-maximum $\Delta H_{1/2}$ and t_0 . The $\phi(t)$ may be calculated, once the two parameters are established, by numerically integrating rather complicated expressions given in the paper of Hennessey *et al.*⁴ In order to compare these theoretical results with our measured line shapes, we have evaluated the theoretical line shapes corresponding to values of t_0 calculated from Eq. (9), using values of J' given in Table IV, and the measured $\Delta H_{1/2}$ value along the chain axis of 16.9 Oe. The values of t_0 for the three approximations are given in Table VI, along with the γ values needed to give $\Delta H_{1/2}$ equal to 16.9 Oe. In Fig. 5 the theoretical curves are plotted corresponding to these three values of t_0 . Clearly, the Tahir-Kheli value for J'/J gives the best agreement with the experimental line profile. Of course, larger values of J'/J would also give agreement with the Lorentzian shape observed. One can say that the Tahir-Kheli prediction for J'/J leads to a calculated line shape which is consistent with our experimental data. A nearest-interchain-neighbor exchange integral j of 0.051 K is thereby obtained.

Note added in proof. The low-temperature calorimetric results on CPC reported here are in fair agreement with those just reported by K. Takeda, Y. Yamamoto, and T. Haseda in Phys. Lett. A **45**, 419 (1973).

ACKNOWLEDGMENTS

Marc Evans and Peter Michelson, both undergraduates at the University of Santa Clara, helped substantially with data reduction and computer calculations from the Hennessey *et al.* theory. The authors are most appreciative to K. Takeda for providing us with his numerical results for the heat capacity of CPC.

*Supported by the National Science Foundation under Grant Nos. GP-29226 and GH-39015.

†Present address: Dept. of Physics, University of California, Santa Barbara, Calif. 93106.

‡Supported by the U. S. Atomic Energy Commission.

¹L. Onsager, Phys. Rev. **65**, 90 (1944).

²G. H. Wannier, Rev. Mod. Phys. **17**, 79 (1945).

³R. R. Bartkowski, M. J. Hennessey, B. Morosin, and P. M. Richards, Solid State Commun. **11**, 405 (1972).

⁴M. J. Hennessey, C. D. McElwee, and P. M. Richards,

- Phys. Rev. B 7, 930 (1973).
- ⁵J. D. Dunitz, Acta Crystallog. 10, 307 (1957).
- ⁶K. Takeda, S. Matsukawa, and T. Haseda, J. Phys. Soc. Jap. 30, 1330 (1971).
- ⁷M. Matsuura, Phys. Lett. A 34, 274 (1971).
- ⁸D. Harker, Z. Kristallog. 93, 136 (1936).
- ⁹T. R. McGuire, and C. T. Lane, Rev. Sci. Instrum. 20, 489 (1949).
- ¹⁰W. Duffy, Jr., D. L. Strandburg, and J. F. Deck, Phys. Rev. 183, 567 (1969).
- ¹¹W. Duffy, Jr., J. F. Dubach, P. A. Pianetta, D. L. Strandburg, and J. F. Deck, J. Chem. Phys. 56, 2555 (1972).
- ¹²E. König and H. L. Schläfer, Z. Phys. Chem. 26, 371 (1960).
- ¹³J. C. Bonner and M. E. Fisher, Phys. Rev. 135, A640 (1964).
- ¹⁴The preliminary result of our measurement of T_N reported in Ref. 4 of 1.135 K is in error and should be corrected to 1.13 K.
- ¹⁵E. Montroll, *Proceedings of the Third Berkeley Symposium on Mathematics, Statistics and Probability* (University of California Press, Berkeley, Calif., 1956), Vol. III.
- ¹⁶H. B. Callen, Phys. Rev. 130, 890 (1963).
- ¹⁷R. A. Tahir-Kheli, Phys. Rev. 132, 689 (1963); R. H. Swendson, Phys. Rev. B 5, 116 (1972).
- ¹⁸H. Abe and K. Ono, J. Phys. Soc. Jap. 11, 947 (1956).
- ¹⁹M. J. Hennessy (private communication).
- ²⁰R. E. Dietz, F. R. Merritt, R. Dingle, D. Hone, B. G. Silbernagel, and P. M. Richards, Phys. Rev. Lett. 26, 1186 (1971).
- ²¹R. A. Tahir-Kheli and D. G. McFadden, Phys. Rev. 182, 604 (1969).